Bio-Impedance Spectroscopy (BIS) Measurement System for Wearable Devices

Bassem Ibrahim*, Drew A. Hall† , Roozbeh Jafari*
* Embedded Signal Processing (ESP) Lab, Texas A&M University, TX
†BioSensors and BioElectronics Group, University of California, San Diego, CA
E-mail: rjafari@tamu.edu

***Abstract*—This paper presents a bio-impedance spectroscopy device for capturing various physiological signals for wearable applications. The system consists of an analog front-end, ADC, and digital signal processing to accurately measure small bio-impedance in the range of 1-120 Ω from the upper arm with an RMSE of 0.07 Ω. The bio-impedance is measured for a wide frequency range, 4 kHz to 120 kHz, in only 150 ms to allow continuous monitoring of rapid physiological activity.**

I. INTRODUCTION

Non-invasive wearable devices are being used extensively to monitor human health and detect diseases as early as possible. Bio-impedance is a non-invasive signal that has many clinical applications such as monitoring congestive heart failure (CHF), diagnosis of the heart and circulatory system [1], hydration, and body composition [2]. The resistance and reactance of bio-impedance are important in the study of biological tissues and to extract their characteristics [3]. Conventionally, bio-impedance is measured across the human body, from hand to hand or hand to foot. Recently, it has become a desirable measurement for wearable medical devices because it is portable, non-invasive, and can be implemented on embedded devices. Modern methods focus on segmental bio-impedance by measuring across parts of the human body (e.g., a single arm or wrist) that are more amenable to wearable devices to enable continuous tracking of physiological activity. Bio-impedance spectroscopy (BIS) is an extension that shows the variation of bio-impedance over a range of frequencies. This paper presents a continuous BIS measurement system for the upper arm that can be integrated into a wearable device.

In previous work, a portable system that measures heart rate using bio-impedance from the forearm was reported [4]; however, it only measured at a single fixed frequency. A system that measures BIS from the chest was reported in [5], but requires placement of the electrodes on the chest which is not as convenient for continuous monitoring compared to other more common arm-worn wearable devices.

The proposed system measures BIS from the upper arm (Fig. 1), which is more comfortable for wearable devices, but comes with several challenges. First, the upper arm bio-impedance is 10× smaller than its whole-body counterpart. The average upper arm bio-impedance is 100 Ω with 100 mΩ variations due to heart activity. Second, to capture the temporal activity, BIS is measured by sweeping the frequency of an AC current source from 4 kHz to 120 kHz and measuring the bio-impedance at each frequency step. Each frequency step is measured in less than

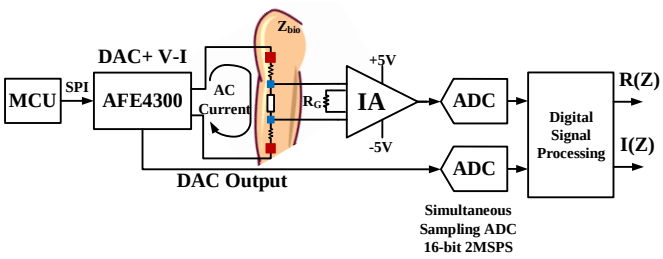

Fig. 1. BIS measurement system block diagram.

4.7 ms to finish a complete BIS measurement in 150 ms. This rapid measurement time allows detection of bio-impedance variations due to fast physiological activities such as heart pumping or respiration, at the cost of increasing the system noise bandwidth. Thus, it becomes challenging to extract the small impedance variations. Lastly, measuring complex impedance requires maintaining an accurate phase relation between the excitation and sense paths. To achieve the target specifications, low noise circuits and tight filtering are used with phase and gain correction to compensate for circuit delays.

The contributions of this paper can be summarized as:

- A BIS system for measurements from small body segments is presented for the first time, which can be integrated into a wearable device. The detailed design and implementation of the circuits and signal processing are discussed to measure very small variations of bio-impedance across wide frequency range in a short time.
- Experimental measurements of upper arm BIS with 4 cm distance between electrodes demonstrating that physiological signals such as heart rate, respiration rate, and muscle contractions can be captured accurately.

The rest of the paper is organized as follows: a brief background is presented in Section II, followed by the description of the analog front-end circuit and the signal processing methods used to implement the BIS system in Section III. Then, Section IV presents measurements from the upper arm and finally, the conclusion.

II. BACKGROUND

The intra-cellular fluid (ICF) and extra-cellular fluid (ECF) of the human body are resistive to the AC current while the cell membrane is capacitive. At DC, the cell membrane blocks current from flowing inside the cell, while at a higher frequency

the current flows through the ICF and ECF, as shown in Fig. 2 (left). The behavior of bio-impedance versus frequency of an AC current can be modeled as an electrical circuit with a cell membrane capacitor C_m in series with ICF resistance R_I in parallel with the ECF resistance R_E, as shown in Fig. 2 (right), known as the Cole-Cole model [6]. A Cole-Cole plot of the bio-impedance across frequency is shown in Fig. 3, which plots the reactance versus resistance at different frequencies. For practical considerations, frequencies between 4 and 120 kHz are used to measure impedance and curve fitting is used to calculate the model parameters (C_m, R_E, and R_I) [7].

III. Methods

The bio-impedance is measured by applying an AC sinusoidal current through a pair of electrodes and sensing the voltage with two different electrodes near the excitation electrode (Kelvin connection) as shown in Fig. 1. The measured voltage is a sinusoidal voltage at the same frequency as the applied current and amplitude modulated by the bio-impedance. Quadrature demodulation is used to obtain the real *R(Z)* and imaginary *I(Z)* components of the impedance by multiplying the sensed signal by the in-phase (*I*) and quadrature (*Q*) carriers.

A. Analog Front-End

The analog front-end consists of a current source, an instrumentation amplifier (IA), and an ADC. The current excitation is generated by a Texas Instruments AFE4300, which has a sinusoidal current source with programmable frequency. The current amplitude is fixed at 375 μA_{RMS} to be compliant with safety standards. The frequency of the AC current is controlled by an internal register written through an SPI bus. An external microcontroller (MCU) is used to send SPI commands to the AFE4300 to sweep the frequency across the target range.

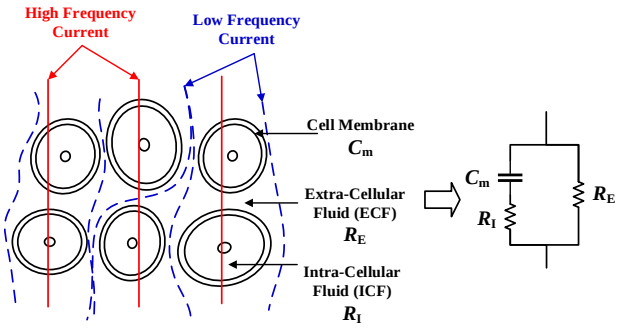

Fig. 2. The flow of current in body cells at a low and high frequency, and the equivalent circuit model.

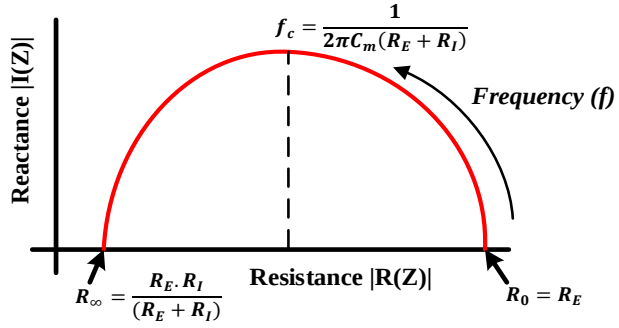

Fig. 3. Cole-Cole plot of bio-impedance.

The system supports measuring bio-impedance in the range of 1 Ω to 120 Ω. Unfortunately, the AFE4300 includes a sense path optimized to measure the bio-impedance of the whole body (~600 Ω), so it does not have enough gain to measure the target impedance range. Thus, an external sense path is used, consisting of an IA followed by a high-speed ADC, and then signal processing in the digital domain. For the IA, the AD8421 with a programmable gain set by an external resistor (R_G) was selected to provide gain up to 40 dB, low noise spectral density of 3.5 nV/√Hz at 1 kHz, and high input impedance compared to the electrode-tissue impedance. The imaginary part of the impedance is extracted from the phase information of the sensed voltage. The IA has 2 MHz bandwidth, which is more than 10× the maximum signal frequency to minimize the phase error between the demodulating signal and sensed voltage that causes impedance error. The IA and DAC outputs are digitized by a 2 channel 16-bit ADC at 2 MSPS.

B. Digital Signal Processing

The ADC outputs are filtered by a bandpass filter around the excitation frequency to remove the DC, 60 Hz power line interference, and any high-frequency spurs or harmonics. The same filter is used for the IA and DAC to avoid introducing any phase error between the two signals before demodulation. The DAC output from the AFE4300 is used as the in-phase carrier for demodulation, while the quadrature carrier is generated from it using the Hilbert transform. Then, the filtered signal is multiplied by the in-phase and quadrature carriers to generate the real and imaginary impedance components, as shown in Fig. 4. The demodulated output is lowpass filtered by a second order filter with a corner frequency of 500 Hz to remove the image frequency and out-of-band noise.

The impedance measurement is sensitive to any gain error or phase error between the signal and carrier during demodulation, which results in an impedance error. Thus, a phase and gain correction step is needed to improve the measurement accuracy. First, the phase and gain errors are estimated by measuring the impedance of a reference resistor with a known value. The error estimation is done as a one-time calibration before system operation. Ideally, the impedance measurement on a pure resistance should have zero phase and amplitude equal to the resistor value (R_{ref}). Thus, the phase error ($\emptyset_{err}$) and gain error (G_{err}) can be estimated at each frequency step from the measured impedance of the reference resistor as:

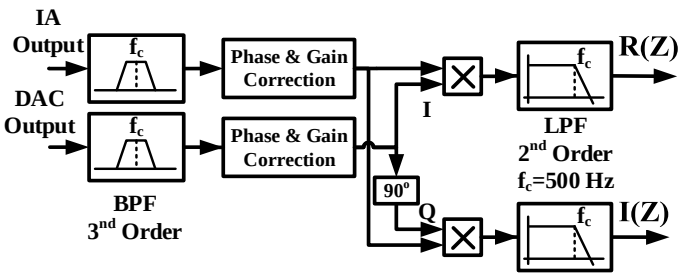

Fig. 4. Digital signal processing block diagram.

$$\emptyset_{\text{err}} = tan^{-1}\frac{I(Z)}{R(Z)} \quad (1)$$

$$G_{\text{err}} = \frac{1}{R_{\text{ref}}}\sqrt{R(Z)^2 + I(Z)^2} \quad (2)$$

Since the phase and gain error vary with frequency, they must be estimated and corrected for every frequency step to ensure accurate impedance measurement across the target frequency range. The phase correction is done in two steps: a coarse phase correction by shifting samples in time which introduces delay of integer multiples of the ADC time step (0.5 µs) and a fine phase correction to compensate for the residual phase error by applying a fractional time delay using an all-pass digital filter with a variable phase shift. The gain correction is implemented by a simple division of the measured impedance by the estimated gain error.

IV. Measurement Resultss

The system was tested using reference resistors and capacitors to check the accuracy for all impedance and frequency range. Fig. 5 shows the linear relationship between the measured resistors values and the reference resistors values from 1 Ω to 120 Ω. The RMSE of the measured impedance was 0.07 Ω. Resistors and capacitors were used to simulate the bio-impedance measured from the upper arm using (R_I=R_E=82.1 Ω, C_m=34.2 nF,) and (R_I=R_E=30.8 Ω, C_m=100.2 nF). Fig. 6 shows the Cole-Cole plot of measured impedance versus the reference resistance, to demonstrate the accuracy of the impedance measurement system for wide range of impedance values ($R(Z)$=40-120 Ω, $I(Z)$=5-30 Ω) and across the frequency range of 4-120 kHz.

The bio-impedance was measured continuously for 30 seconds from the human body, encompassing 200 BIS measurements using two different electrode positions. The electrodes were placed across and along the upper arm, as shown in Fig. 7. The Cole-Cole plot of the bio-impedance measured along the upper arm across frequency is shown in Fig. 8. The electrodes were placed 1, 2 and 3 cm apart successively. The real and imaginary parts of the bio-impedance increased as the electrode separation increased since a larger volume of tissue is measured corresponding to a higher impedance.

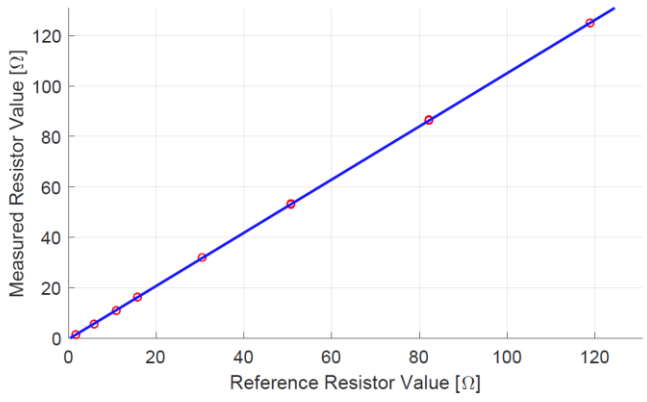

Fig.5. Plot showing measured vs. reference resistances from 1-120 Ω.

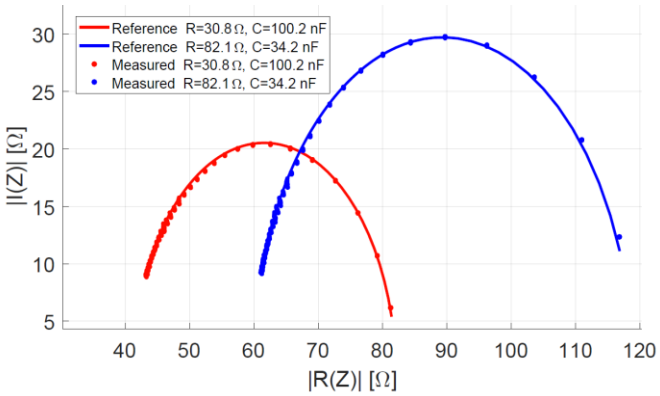

Fig. 6. Cole-Cole plot of measured vs. reference impedances

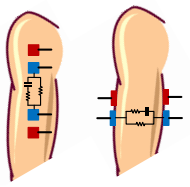

Fig. 7. Placement of the excitation (red) and sensing (blue) electrodes along (left) and across (right) upper arm.

Respiration and heart activity cause small changes in the bio-impedance over time. These changes are more significant in the real part compared to the imaginary part. The real part of the bio-impedance was measured from the upper arm for the frequency range from 8 to 43 kHz for 30 seconds as shown in Fig. 9. An accelerometer was fixed on the chest to provide a reference for the actual respiration rate from chest movements. The acceleration was simultaneously measured with bio-impedance to show the direct correlation between them. There was variation in bio-impedance of ~1.5 Ω due to respiration, as shown in Fig. 10(a). In addition, the bio-impedance had superimposed variations of around 0.3 Ω due to heart activity, which is shown in Fig. 10(b) after removing the respiration using a highpass filter. These small bio-impedance variations were used to detect the average heart rate, which was verified by comparison with the reference chest ECG signal captured simultaneously as shown in Fig. 10(c).

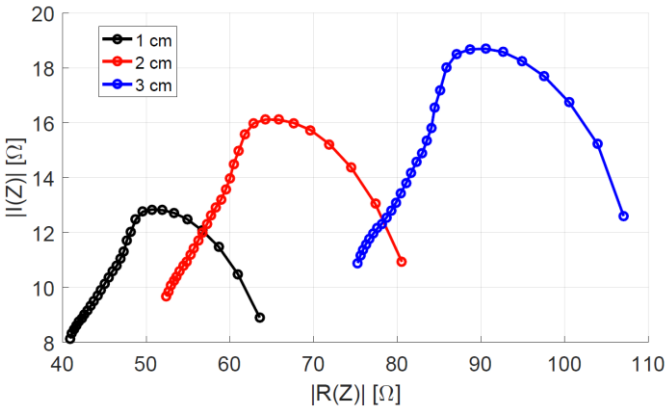

Fig. 8. Cole-Cole plot of bio-impedance along upper arm for different electrode distances (1, 2, and 3 cm).

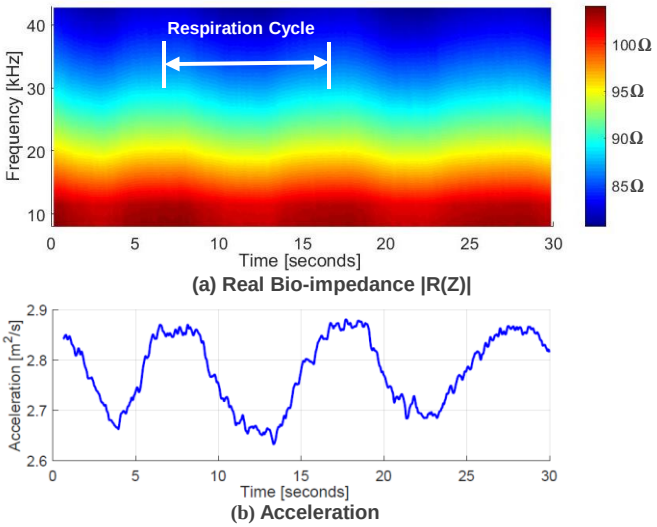

Fig. 9. Respiration rate from simultaneous measurement of: (a) upper arm bio-impedance $|R(Z)|$ from 8 to 43 kHz and (b) accelerometer on the chest.

To demonstrate a larger change of bio-impedance over time, measurements were done on the upper arm while contracting and relaxing arm bicep muscles for intervals of 5 seconds repeatedly. Fig. 11 shows the real and imaginary parts of bio-impedance versus frequency and time with clear variations in time due to muscle contractions.

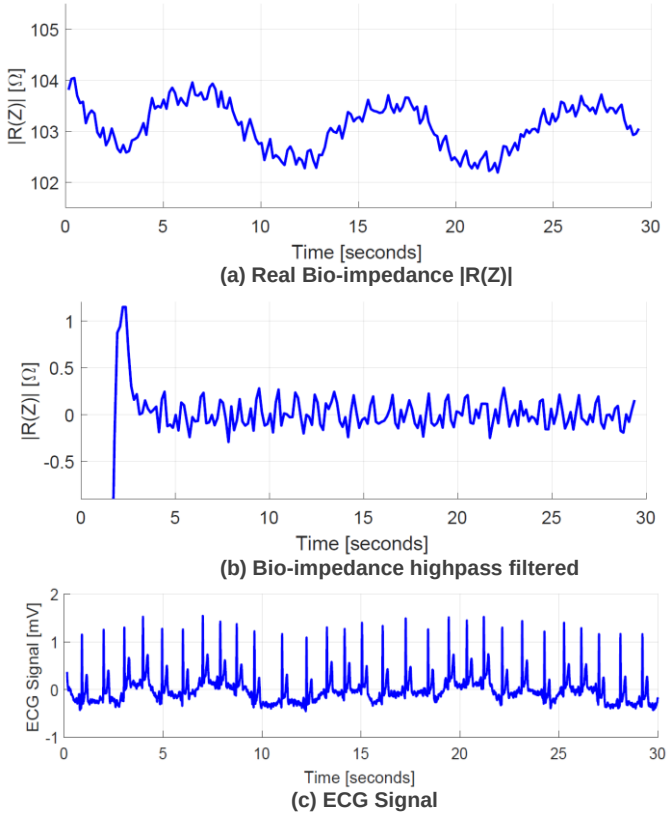

Fig. 10. Time course plots showing (a) upper arm bio-impedance $|R(Z)|$ at 8 kHz with variations due to respiration and heart pumping, (b) heart rate after removing the respiration, and (c) simultaneous measurement of ECG signal from the chest.

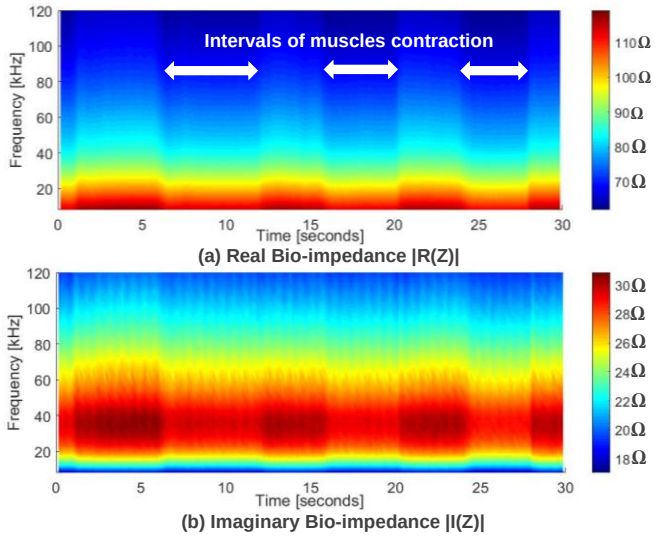

Fig. 11. Muscles contractions are shown by the marked time intervals of the upper arm bio-impedance across the whole frequency range.

V. Conclusions

This paper presents an accurate measurement system for bio-impedance spectroscopy from the upper arm with RMSE of 0.07 Ω for the frequency range from 4 kHz to 120 kHz in only 125 ms to allow continuous time monitoring of BIS. The measurements of reference impedances prove the system accuracy. Experimental measurements of BIS are shown which are used to detect different physiological activities. This system demonstrates the continuous monitoring of BIS from the upper arm which can be integrated into a wearable device.

References

[1] T. K. Bera, "Bioelectrical Impedance Methods for Noninvasive Health Monitoring: A Review," *Journal of Medical Engineering*, vol. 2014, pp. 1-28, 2014.

[2] J. R. Matthie, "Bioimpedance measurements of human body composition: critical analysis and outlook," *Expert Review of Medical Devices*, vol. 5, pp. 239-261, 2008.

[3] D. A. Dean, T. Ramanathan, D. Machado and R. Sundararajan, "Electrical impedance spectroscopy study of biological tissues," *Journal of Electrostatics*, vol. 66, pp. 165-177, mar 2008.

[4] M. C. Cho, J. Y. Kim and S. Cho, "A bio-impedance measurement system for portable monitoring of heart rate and pulse wave velocity using small body area," in *2009 IEEE International Symposium on Circuits and Systems*, 2009.

[5] J. Xu, P. Harpe, J. Pettine, C. V. Hoof and R. F. Yazicioglu, "A low power configurable bio-impedance spectroscopy (BIS) ASIC with simultaneous ECG and respiration recording functionality," in *European Solid-State Circuits Conference (ESSCIRC), ESSCIRC 2015 - 41st*, 2015.

[6] U. G. Kyle, I. Bosaeus, A. D. D. Lorenzo, P. Deurenberg, M. Elia, J. M. Gómez, B. L. Heitmann, L. Kent-Smith, J.-C. Melchior, M. Pirlich, H. Scharfetter, A. M. W. J. Schols and C. Pichard, "Bioelectrical impedance analysis—part I: review of principles and methods," *Clinical Nutrition* , vol. 23, pp. 1226-1243, 2004.

[7] F. Seoane, J. Ferreira, J. J. Sanchéz and R. Bragós, "An analog front-end enables electrical impedance spectroscopy system on-chip for biomedical applications," *Physiological Measurement*, vol. 29, p. S267, 2008.